Inflammasome-independent IL-1β mediates autoinflammatory disease in Pstpip2-deficient mice

Suzanne L. Cassel[a,b,c,1], John R. Janczy[a,c], Xinyu Bing[d], Shruti P. Wilson[b], Alicia K. Olivier[e], Jesse E. Otero[f], Yoichiro Iwakura[g,h], Dmitry M. Shayakhmetov[i], Alexander G. Bassuk[d], Yousef Abu-Amer[j], Kim A. Brogden[k], Trudy L. Burns[d,l], Fayyaz S. Sutterwala[a,b,c,m,1], and Polly J. Ferguson[d,1,2]

[a]Inflammation Program, [b]Department of Internal Medicine, [c]Graduate Program in Immunology, [d]Department of Pediatrics, [e]Department of Pathology, [f]Department of Orthopedics, [k]Dows Institute for Dental Research and Department of Periodontics, College of Dentistry, and [l]Department of Epidemiology, University of Iowa, Iowa City, IA 52242; [g]Research Institute for Biomedical Sciences, Tokyo University of Science Yamasaki 2669, Noda, Chiba 278-0022, Japan; [h]Core Research for Evolutional Science and Technology, Japan Science and Technology Agency, Saitama 332-0012, Japan; [i]Division of Medical Genetics, Department of Medicine, University of Washington, Seattle, WA 98195; [j]Department of Orthopedics, Washington University School of Medicine, St. Louis, MO 63110; and [m]Veterans Affairs Medical Center, Iowa City, IA 52241

Edited by Ruslan Medzhitov, Yale University School of Medicine, New Haven, CT, and approved December 13, 2013 (received for review October 3, 2013)

Chronic recurrent multifocal osteomyelitis (CRMO) is a human autoinflammatory disorder that primarily affects bone. Missense mutation (L98P) of proline-serine-threonine phosphatase-interacting protein 2 (Pstpip2) in mice leads to a disease that is phenotypically similar to CRMO called chronic multifocal osteomyelitis (cmo). Here we show that deficiency of IL-1RI in cmo mice resulted in a significant reduction in the time to onset of disease as well as the degree of bone pathology. Additionally, the proinflammatory cytokine IL-1β, but not IL-1α, played a critical role in the pathology observed in cmo mice. In contrast, disease in cmo mice was found to be independent of the nucleotide-binding domain, leucine-rich repeat-containing family, pyrin domain-containing 3 (NLRP3) inflammasome as well as caspase-1. Neutrophils, but not bone marrow-derived macrophages, from cmo mice secreted increased IL-1β in response to ATP, silica, and *Pseudomonas aeruginosa* compared with neutrophils from WT mice. This aberrant neutrophil response was sensitive to inhibition by serine protease inhibitors. These results demonstrate an inflammasome-independent role for IL-1β in disease progression of cmo and implicate neutrophils and neutrophil serine proteases in disease pathogenesis. These data provide a rationale for directly targeting IL-1RI or IL-1β as a therapeutic strategy in CRMO.

chronic osteomyelitis | innate immunity

Chronic recurrent multifocal osteomyelitis (CRMO) is a sterile inflammatory disorder that affects children and presents with bone pain due to sterile osteomyelitis (1). The etiology of the disease is unknown, but it is associated with Crohn disease, inflammatory arthritis, and psoriasis in affected individuals and their close relatives, suggesting a shared pathophysiology and supporting a genetic contribution to disease (2). There are two autosomal recessive disorders that present with neonatal- or infant-onset sterile osteitis that are histologically similar to the bone disease in CRMO and clinically improve with IL-1 blockade (3, 4). Majeed syndrome, caused by mutations in *LPIN2*, presents with CRMO, congenital dyserythropoietic anemia, and sterile neutrophilic dermatosis (5). Deficiency of the IL-1 receptor antagonist (DIRA) is caused by mutations in *IL1RN*, which encodes the IL-1 receptor antagonist (3), resulting in dysregulation of the IL-1 pathway. Affected individuals present with neonatal-onset cutaneous pustulosis, marked elevation of inflammatory markers, sterile multifocal osteitis, and periostitis (3).

There are two autosomal recessive murine models of CRMO both due to mutations in *proline-serine-threonine interacting protein 2* (*Pstpip2*) (6–8). The mutation (L98P) present in the chronic multifocal osteomyelitis (cmo) model results in no detectable expression of Pstpip2, a protein expressed predominantly in the cells of the myeloid lineage, and leads to disease that resembles human CRMO (6, 9). The development of osteomyelitis in the cmo mouse is hematopoietically driven and develops in the absence of lymphocytes, consistent with an autoinflammatory mechanism of disease (9). Although it is known that cmo mice have a dysregulated innate immune system, it is not clear what inflammatory pathway is critical for disease.

Mutations within *NLRP3* (also known as NALP3 or cryopyrin) are associated with the autoinflammatory Muckle-Wells syndrome, familial cold autoinflammatory syndrome, and neonatal-onset multisystem inflammatory disease, collectively known as cryopyrin-associated periodic syndrome (10). These *NLRP3* mutations result in a constitutively active form of NLRP3 that leads to increased inflammasome activation with a resultant increase in secretion of IL-1β (10). A diverse array of agonists has been identified that are capable of activating NLRP3, which results in the assembly of the NLRP3 inflammasome composed of NLRP3, the adaptor molecule apoptosis-associated speck-like protein containing a CARD (ASC), and caspase-1 (11). The activation of the inflammasome leads to the activation of caspase-1, with the resultant processing of pro-IL-1β and pro-IL-18 to their mature and secreted forms (12). However, the role of the NLRP3 inflammasome in the pathogenesis of cmo remains unknown.

Given the evidence that IL-1 is important in the pathogenesis of sterile bone inflammation in humans (3, 4), we investigated the role of IL-1 in the pathogenesis of sterile osteomyelitis in the cmo mouse. Here we demonstrate that deficiency of IL-1RI (interleukin-1 receptor type I) or IL-1β in cmo mice resulted in

Significance

Chronic recurrent multifocal osteomyelitis (CRMO) is a human disorder of the innate immune system that causes bone inflammation that mimics infectious osteomyelitis. There is a spontaneous mutant mouse model of the disease that is caused by homozygous mutations in the gene *Pstpip2*. Our studies show that bone inflammation in this model is mediated by the cytokine IL-1β, but that the disease is independent of the nucleotide-binding domain, leucine-rich repeat-containing family, pyrin domain-containing 3 (NLRP3) inflammasome and caspase-1, which is different from most other IL-1–mediated disorders. Further, we implicate neutrophils and neutrophil serine proteases in disease pathogenesis. These data provide a rationale for directly targeting the IL-1 receptor or IL-1β as a therapeutic strategy in CRMO.

Author contributions: S.L.C., J.R.J., J.E.O., A.G.B., F.S.S., and P.J.F. designed research; S.L.C., J.R.J., X.B., S.P.W., A.K.O., J.E.O., K.A.B., F.S.S., and P.J.F. performed research; S.L.C., Y.I., D.M.S., Y.A.-A., F.S.S., and P.J.F. contributed new reagents/analytic tools; S.L.C., J.R.J., X.B., A.K.O., J.E.O., A.G.B., T.L.B., F.S.S., and P.J.F. analyzed data; and S.L.C., J.R.J., A.G.B., F.S.S., and P.J.F. wrote the paper.

The authors declare no conflict of interest.

This article is a PNAS Direct Submission.

[1]S.L.C., F.S.S., and P.J.F. contributed equally to this work.

[2]To whom correspondence should be addressed. E-mail: polly-ferguson@uiowa.edu.

delayed onset of disease and an attenuation of disease severity. In contrast, disease progression in cmo mice was found to be independent of the NLRP3 inflammasome, and in vitro findings support a role for neutrophil serine proteases in the abnormally increased secretion of IL-1β. Taken together these data demonstrate an inflammasome-independent role for the IL-1 pathway in the disease pathogenesis of cmo.

Results and Discussion

Pstpip2-Deficient cmo Mice Have Increased Proinflammatory Cytokines in Vivo. The role of the IL-1 pathway in the disease pathogenesis of cmo is largely unknown. To determine the contribution of inflammatory mediators in vivo we assessed tissue cytokine levels in the tails of symptomatic cmo mice. As expected, WT mice had minimal inflammatory cytokines detected within tail homogenates (Fig. 1 *A* and *B*). IL-1β levels were significantly elevated, whereas IL-1α levels also trended toward being increased in cmo mice (Fig. 1*A*). Because previous studies have demonstrated elevated serum levels of proinflammatory cytokines in cmo mice, we investigated these cytokines in tail homogenates. Consistent with these previous studies, we observed elevated granulocyte colony stimulating factor (G-CSF), IL-12 p40, macrophage inflammatory protein (MIP)-1α, and MIP-1β levels in tails of cmo mice (Fig. 1*B*) (9).

IL-1RI Deficiency Protects cmo Mice from Developing Bone Pathology. IL-1α and IL-1β are both able to bind to IL-1RI; after recruitment of the coreceptor chain, IL-1RAcP, signaling culminates in activation of NF-κB. To determine the role of IL-1RI in cmo pathogenesis, cmo mice were crossed with IL-1RI–deficient mice. By 21 wk of age all cmo.*IL-1RI*$^{+/-}$ mice developed tail kinks and hind foot deformities, as well as histological and radiologic evidence of osteomyelitis (Fig. 2 *A–E*). In contrast, none of the cmo.*IL-1RI*$^{-/-}$ mice developed clinical or histological evidence of disease even at 180 d of age (Fig. 2 *A–E*). The lack of IL-1RI also abrogated the increased number and size of osteoclasts seen in cmo mice in vivo (Fig. 2 *F* and *G*). These data suggest that signaling through the IL-1RI plays an important role in mediating cmo disease pathogenesis.

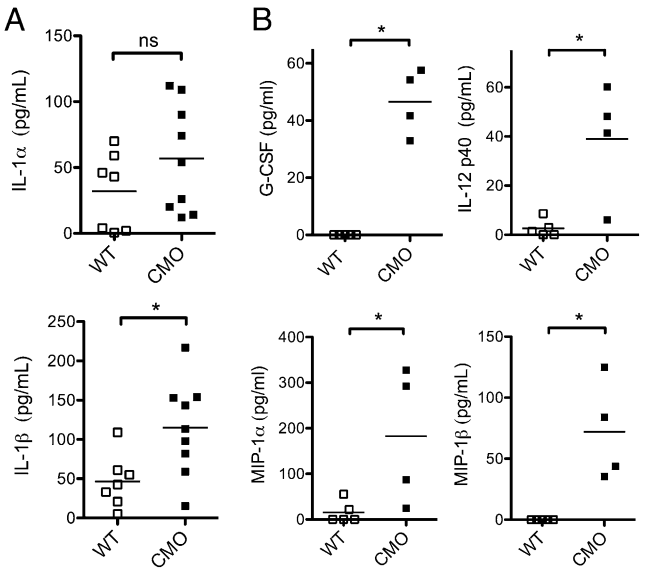

Fig. 1. cmo mice have elevated proinflammatory cytokines in vivo. (*A*) Tail homogenates from WT ($n = 7$) or cmo mice ($n = 9$) were assessed for IL-1α and IL-1β via ELISA. (*B*) Tail homogenates from WT ($n = 5$) or cmo mice ($n = 4$) were assessed for the indicated cytokines via multiplex assay. ns, not significant, $^*P < 0.05$ by two-tailed Mann-Whitney test.

IL-1β Deficiency, but Not IL-1α Deficiency, Results in Diminished Bone Inflammation in cmo Mice. Because both IL-1α and IL-1β signal through the IL-1RI we crossed mice deficient in either IL-1α or IL-1β with cmo mice to determine their individual contribution to cmo pathology. No significant difference in the time to onset of disease or the degree of tail bone destruction and inflammation was observed in cmo.*IL-1α*$^{-/-}$ mice compared with control cmo.*IL-1α*$^{+/-}$ mice (Fig. 3 *A–C*). In contrast, cmo.*IL-1β*$^{-/-}$ mice were significantly protected from developing disease; at 85 d of age only 17% of cmo.*IL-1β*$^{-/-}$ mice had developed clinical signs of disease, in comparison with 88% of control cmo.*IL-1β*$^{+/-}$ mice (Fig. 3*D*). Histological analysis of tail bones of cmo.*IL-1β*$^{-/-}$ mice at ∼180 d of age revealed structurally normal bone with minimal inflammatory infiltrates (Fig. 3 *E* and *F*). Although cmo.*IL-1β*$^{-/-}$ mice displayed significantly diminished disease compared with control cmo.*IL-1β*$^{+/-}$ mice they did not fully recapitulate the lack of disease observed in cmo.*IL-1RI*$^{-/-}$ mice, suggesting that IL-1α and IL-1β may have synergistic affects in mediating cmo disease. Alternatively, in addition to IL-1α and IL-1β other unknown inflammatory mediators that signal through the IL-1RI may contribute to cmo disease.

Disease Progression in cmo Mice Is Independent of the NLRP3 Inflammasome. In response to cellular stress the NLRP3 inflammasome activates caspase-1, resulting in the processing and secretion of the proinflammatory cytokine IL-1β. To determine the contribution of the NLRP3 inflammasome to cmo pathogenesis, cmo mice were crossed with either NLRP3-, ASC-, or caspase-1–deficient mice, and clinical disease was assessed over time. In contrast to cmo.*IL-1RI*$^{-/-}$ and cmo.*IL-1β*$^{-/-}$ mice, cmo mice deficient in *Nlrp3*, *Asc*, or *caspase-1* developed disease at similar rates to cmo mice heterozygous for *Nlrp3*, *Asc*, or *caspase-1* (Fig. 4 *A–C*). The finding that cmo disease was caspase-1 independent yet IL-1β dependent was unexpected and implicates an alternative cleavage mechanism for pro-IL-1β in cmo pathogenesis other than the known inflammasome pathways, all of which are reliant upon activated caspase-1.

Multiple proteases, including caspase-1, can convert pro-IL-1β into the biologically active mature IL-1β (13–20). Specificity of enzymatic cleavage sites and resultant changes in molecular weight can be used to help determine candidate proteases used that cleave particular substrates. We analyzed by immunoblot the IL-1β that was isolated from hind paw homogenates of 12- to 16-wk-old WT, cmo, cmo.*IL-1RI*$^{-/-}$, and cmo.*Casp1*$^{-/-}$ mice (Fig. 4*D*). Consistent with ELISA results (Fig. 1*A*), we observed the presence of increased pro-IL-1β in homogenates from cmo mice compared with WT mice (Fig. 4*D*). Interestingly hind paw homogenates from cmo.*Casp1*$^{-/-}$ mice displayed similar IL-1β cleavage products compared with cmo mice (Fig. 4*D*). These data suggest that although the NLRP3 inflammasome and caspase-1 do not play a role in cmo disease pathogenesis, pro-IL-1β may be processed by a protease other than caspase-1.

Neutrophils from cmo Mice Secrete Increased IL-1β. The pathology observed in cmo mice in vivo was driven in part by IL-1β signaling through the IL-1RI. To determine the cell type responsible for IL-1β secretion in cmo mice, we stimulated lipopolysaccharide (LPS)-primed cmo bone marrow (BM) with known inflammasome agonists. BM cells from cmo mice secreted significantly more IL-1β in response to adenosine triphosphate (ATP), silica, and *Pseudomonas aeruginosa* compared with BM from WT mice (Fig. 5 *A–C*). Unlike BM cells from cmo mice, cmo BM-derived macrophages (BMDMs) did not secrete increased amounts of IL-1β in response to ATP or silica (Fig. 5*D*). Caspase-1 activation involves autocatalytic processing of the 45-kDa procaspase-1 to generate two subunits, p20 and p10. Silica stimulation of LPS-primed WT and cmo macrophages resulted in similar activation of caspase-1, as detected by immunoblot by the appearance of the caspase-1

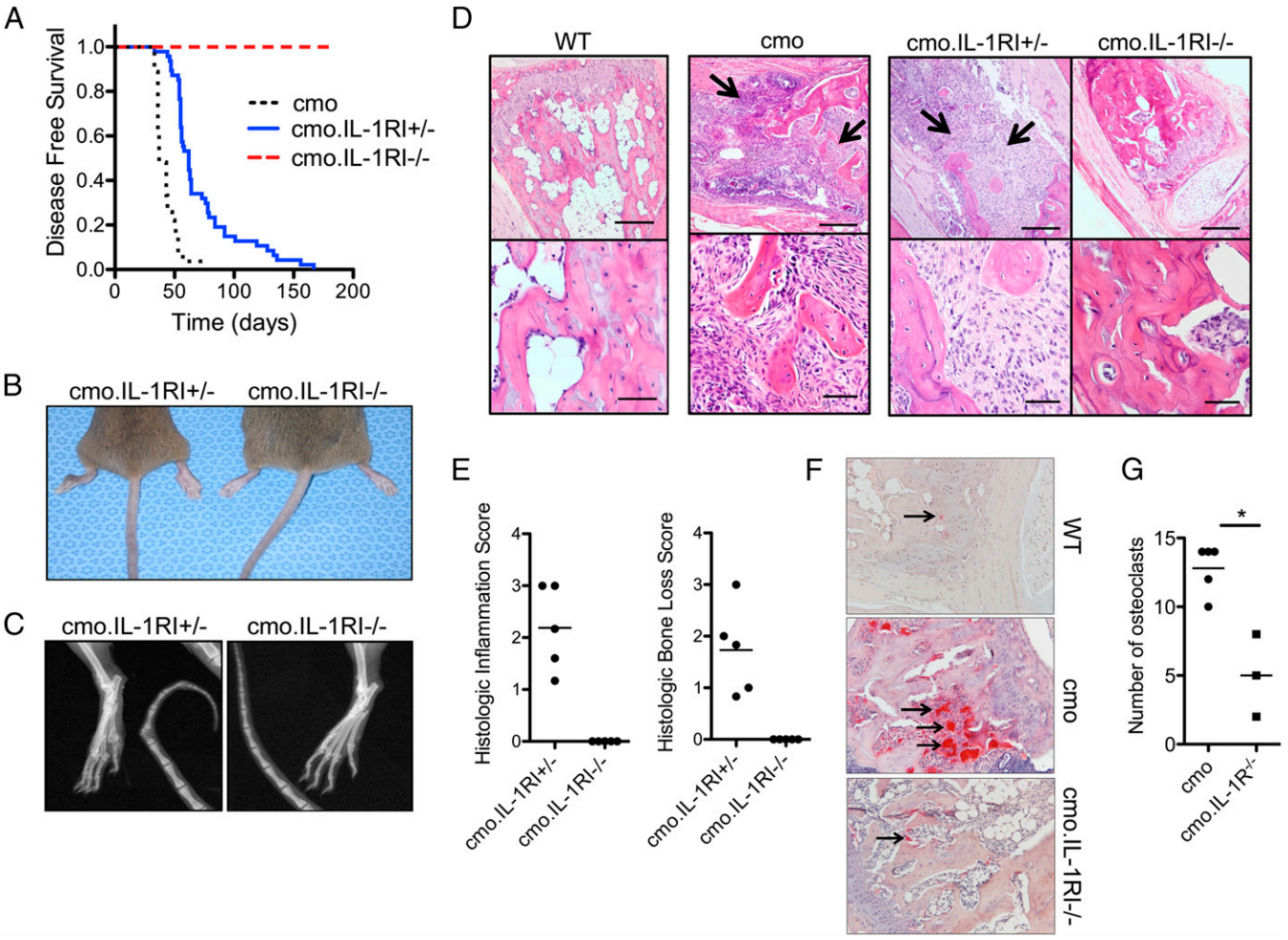

Fig. 2. IL-1RI–deficient mice are protected from developing cmo pathology. (*A*) Kaplan-Meier disease-free survival curves for cmo ($n = 27$), cmo.*IL-1RI*$^{+/-}$ ($n = 48$), and cmo.*IL-1RI*$^{-/-}$ ($n = 49$) mice. Test of equality over the three groups (log–rank $P < 0.0001$; Bonferroni-adjusted pairwise survival curve comparisons, each $P < 0.0005$). (*B* and *C*) Representative tail kinks and foot deformities in a 3-mo-old cmo.*IL-1RI*$^{+/-}$ mouse in comparison with a littermate *cmo.IL-1RI*$^{-/-}$ mouse by gross (*B*) and radiological (*C*) examination. (*D*) Representative fixed decalcified tail bone from WT, cmo, cmo.*IL-1RI*$^{+/-}$, and cmo.*IL-1RI*$^{-/-}$ sectioned and stained with H&E. In the cmo and cmo.*IL-1RI*$^{+/-}$ sections there is loss of trabecular and cortical bone, with fibrosis and infiltration of macrophages, lymphocytes, and neutrophils (arrows). In contrast, the section from the cmo.*IL-1RI*$^{-/-}$ mouse shows normal bone with no inflammation. (Scale bars, *Upper*, 200 μm; *Lower*, 50 μm.) (*E*) Histological scoring for severity of inflammation and bone loss was performed on tail bones from cmo mice lacking IL-1RI compared with heterozygous controls ($n = 5$ per group). (*F*) Histologic sections of tail vertebrae from WT, cmo, and cmo.*IL-1RI*$^{-/-}$ mice stained for TRAP, a marker for osteoclasts (arrows). (*G*) Number of osteoclasts per 400× field per mouse was scored using ImageJ software ($n = 5$ for cmo, $n = 3$ for cmo.*IL-1RI*$^{-/-}$). *$P = 0.033$ by two-tailed Mann-Whitney test.

p10 cleavage product (Fig. 5*E*). However, BM from both WT and cmo mice failed to induce the activation of caspase-1 in response to silica (Fig. 5*E*).

To determine the specific cell type responsible for the elevated IL-1β production observed in cmo BM, we next isolated BM neutrophils from WT and cmo mice and stimulated them with the NLRP3 agonist silica. Consistent with our findings with cmo BM, we observed increased IL-1β secretion from purified cmo neutrophils in response to silica compared with WT neutrophils (Fig. 5*F*). The increased secretion of IL-1β from cmo BM was sensitive to inhibition of serine proteases with the pharmacologic inhibitor diisopropylfluorophosphate (DFP) (Fig. 5*G*) but not the caspase-1 inhibitor z-YVAD-fmk (Fig. 5*H*). These results demonstrate a caspase-1–independent role for IL-1β in disease progression of cmo and implicate neutrophil serine proteases in disease pathogenesis.

In monocytic cells, the processing of pro-IL-1β into its biologically active 17-kDa mature form is caspase-1 dependent. However, a number of proteases, including neutrophil serine proteases, matrix metalloproteinases, and chymases derived from mast cells, can cleave pro-IL-1β at distinct cleavage sites to produce biologically active IL-1β (13–20). Neutrophils have been shown to play an important role in the pathogenesis of numerous sterile inflammatory disorders and are a prominent cell type seen in the inflamed bone in the cmo mouse. Neutrophil serine proteases in particular have been shown to produce and release IL-1β in vivo in several murine models of sterile inflammation, including in the K/BxN serum transfer model of inflammatory arthritis, monosodium urate crystal-induced peritonitis, and in antimyeloperoxidase antibody-induced necrotizing crescentic glomerulonephritis (16, 21, 22). Our findings here implicate neutrophil serine proteases in the pathogenesis of cmo. Further studies will be required to delineate the particular serine protease involved; candidate proteases include neutrophil elastase, cathepsin G, cathepsin C, and proteinase 3.

Children with CRMO as a subphenotype of DIRA and Majeed syndrome improve with IL-1 blockade (3–5). In addition, there are recent reports describing the use of IL-1 blockade for

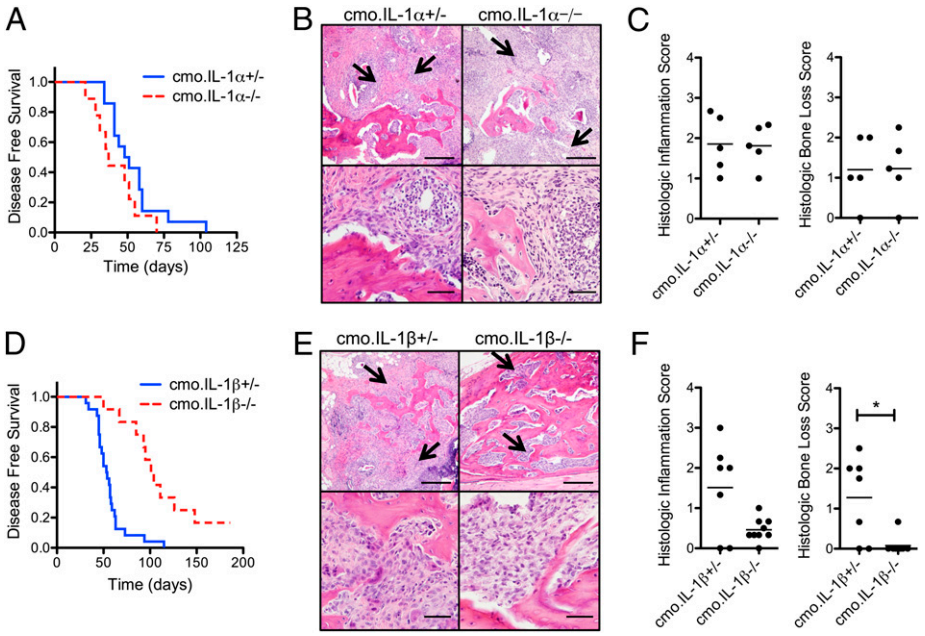

Fig. 3. Mice deficient in IL-1β, but not IL-1α, are protected from developing cmo disease. (*A*) Kaplan-Meier disease-free survival curves for cmo.*IL-1α*$^{+/-}$ ($n = 14$) and cmo.*IL-1α*$^{-/-}$ ($n = 9$); $P = 0.12$ by log–rank test. (*B*) Representative fixed decalcified tail bone sections from cmo.*IL-1α*$^{+/-}$ and cmo.*IL-1α*$^{-/-}$ mice stained with H&E. Images are representative of the most severe lesions observed in each genotype. Loss of trabecular and cortical bone with fibrosis and infiltration of macrophages, lymphocytes, and neutrophils is indicated by arrows. (Scale bars, *Upper*, 200 μm; *Lower*, 50 μm.) (*C*) Histological scoring for severity of bone loss and inflammation was performed on tails from cmo.*IL-1α*$^{+/-}$ and cmo.*IL-1α*$^{-/-}$ mice. (*D*) Kaplan-Meier disease-free survival curves for cmo.*IL-1β*$^{+/-}$ ($n = 24$) and cmo.*IL1β*$^{-/-}$ ($n = 12$); $P < 0.0001$ by log–rank test. (*E*) Representative fixed decalcified tail bone sections from cmo.*IL-1β*$^{+/-}$ and cmo.*IL-1β*$^{-/-}$ mice stained with H&E as described above. (*F*) Histological scoring for severity of bone loss and inflammation on tails from cmo.*IL-1β*$^{+/-}$ and cmo.*IL-1β*$^{-/-}$; *$P = 0.0125$ by two-tailed Mann-Whitney test.

the treatment of sporadic cases of pediatric- and adult-onset CRMO. One adult with CRMO subsequently developed Still disease. The Still manifestations were treated with anakinra, and the bone lesions completely resolved (23). Another adult with CRMO as part of SAPHO (synovitis, acne, pustulosis, hyperostosis and osteitis) syndrome was treated with anakinra, resulting in both clinical and radiologic improvement in her bone disease (24). A third case reported transient resolution of bone disease in a 6-y-old with CRMO treated with anakinra (25). Taken together these clinical reports, along with the findings presented here, demonstrate the importance of the IL-1 pathway in the development of bone inflammation and further provide rationale for a therapeutic trial of IL-1R blockade in CRMO.

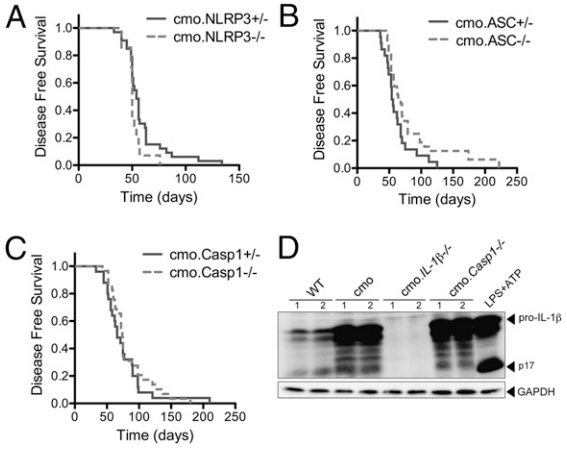

Fig. 4. Disease in the cmo mouse is inflammasome independent. (*A*) Kaplan-Meier disease curves for cmo.*NLRP3*$^{+/-}$ ($n = 25$) and cmo.*NLRP3*$^{-/-}$ ($n = 14$); log–rank test $P = 0.03$. (*B*) Disease-free survival curve for cmo.*ASC*$^{+/-}$ ($n = 22$) and cmo.*ASC*$^{-/-}$ ($n = 29$); log–rank test $P = 0.16$. (*C*) Disease-free survival curve for cmo.Casp*1*$^{+/-}$ ($n = 25$) and cmo.Casp*1*$^{-/-}$ ($n = 28$); log–rank test $P = 0.32$. (*D*) Hind paw homogenates from WT, cmo, cmo.*IL1β*$^{-/-}$, and cmo.Casp*1*$^{-/-}$ mice were immunoblotted for IL-1β and GAPDH. A positive control from LPS-primed BMDMs stimulated with ATP (LPS+ATP) is included to demonstrate caspase-1–mediated IL-1β cleavage. Each lane represents an individual mouse.

Materials and Methods

Mice. The NLRP3-, ASC-, caspase-1-, IL-1RI-, IL-1α-, IL-1β-deficient mice (26–30), and Pstpip2-deficient cmo mice (C.Cg-*Pstpip2*$^{cmo/J}$) (6, 8) have been described previously. BALB/cByJ and BALB/cJ mice (Jackson Laboratories) were used as controls for in vitro studies as indicated. Double-mutant mice were made by crossing C.Cg-*Pstpip2*$^{cmo/J}$ mice (on a BALB/cAnPt background) with NLRP3-, ASC-, caspase-1-, IL-1RI-, IL-1α-, or IL-1β–deficient mice on a C57BL/6 background. The offspring were then intercrossed to obtain homozygote mice deficient in Pstpip2 and the additional molecule of interest or littermate controls heterozygous for the molecule of interest. The University of Iowa Institutional Animal Care and Use Committee approved all protocols used in this study.

Disease Scoring and Tissue Homogenates. Severity of disease was assessed twice weekly after 4 wk of age and assigned according to the proportion of the tail that was diseased as follows: 0 = normal tail, 1 = swelling and deformity of the distal 1/3, 2 = disease involving the distal 1/2, 3 = disease involving the distal 2/3, and 4 = disease involving the whole tail. Equal weights of distal de-skinned tail segments were snap frozen with liquid nitrogen and homogenized in 50 mM Tris, 5 mM EDTA, 150 mM NaCl, and 1% Triton X-100 containing a protease inhibitor mixture (Roche); debris was pelleted, and the supernatant was assessed via ELISA. Antibody pairs for the IL-1α and IL-1β ELISAs were from eBiosciences and R&D Systems, respectively, and will detect both the pro- and mature forms of these cytokines. G-CSF, IL-12 p40, MIP-1α, and MIP-1β were assessed by Luminex assay (R&D Systems). Hind paws were harvested, snap-frozen in liquid nitrogen, and homogenized in RIPA lysis buffer supplemented with complete protease inhibitor mixture (Roche) and PhosSTOP (Roche). Debris was pelleted and lysates assessed by immunoblot.

Histology and Histologic Scoring. Tail bones were placed in neutral buffered formalin followed by decalcification in EDTA. After decalcification bones

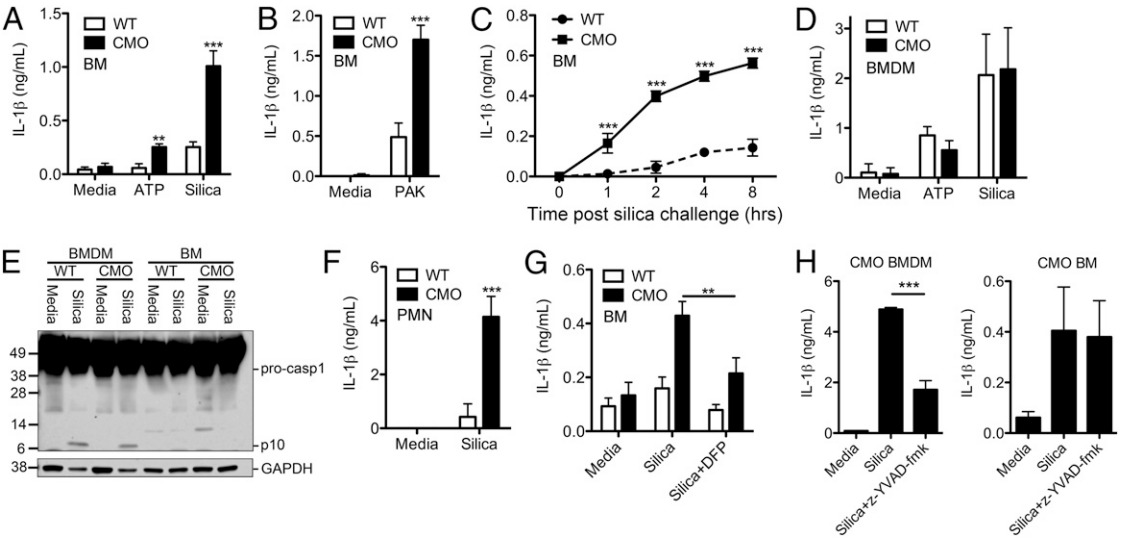

Fig. 5. Neutrophils from cmo mice produce elevated IL-1β in vitro. (*A–C*) BM cells from WT or cmo mice were LPS-primed and then stimulated with either ATP (5 mM), silica (50 μg/cm^2), or *P. aeruginosa* PAK strain at a multiplicity of infection of 1:1; culture supernatants were collected 5 h later, or at the indicated time, and IL-1β release measured by ELISA. (*D*) BMDMs from WT and cmo mice were LPS-primed, followed by stimulation with either ATP or silica for 6 h, after which supernatants were assessed for IL-1β via ELISA. (*E*) Lysates from LPS-primed WT or cmo BMDMs and BM cells stimulated with silica for 5 h were immunoblotted with antibodies against the p10 subunit of caspase-1 and GAPDH. (*F*) Neutrophils (PMN) from WT and cmo mice were isolated by Percoll gradient centrifugation, LPS-primed, and stimulated with silica for 5 h; IL-1β secretion into culture supernatants was determined by ELISA. (*G*) BM cells from WT or cmo mice were LPS-primed, pretreated for 20 min with the serine protease inhibitor DFP, and then challenged with silica. Supernatants were collected 5 h later and were assessed for IL-1β via ELISA. (*H*) BMDMs and BM from cmo mice were LPS-primed, pretreated with the caspase-1 inhibitor z-YVAD-fmk (10 μM) for 30 min, and then challenged with silica. Supernatants were collected 5 h later and assessed for IL-1β via ELISA. Determinations were performed in triplicate and expressed as the mean ± SD (*B–D*, *F–H*); results are representative of two (*B*, *E*, *G*, and *H*) and three (*C*, *D*, and *F*) separate experiments. Data represent the mean ± SEM of four separate experiments (*A*). $^{**}P < 0.01$, $^{***}P < 0.001$ by two-way ANOVA with a Bonferroni posttest (*A–D*, *F*). $^{**}P < 0.01$ by Student *t* test (*G*), $^{***}P < 0.001$ by one-way ANOVA (*H*).

were embedded in paraffin. Tissues were cut at 4 μm and stained with either H&E or tartrate-resistant acid phosphatase (TRAP). Histological scoring for severity of inflammation and bone loss was performed on H&E sections of tail bones. Bone inflammation was scored for each vertebral body according to the percentage of the BM space containing inflammatory cells; 0 (no inflammation), 1 (<25%), 2 (25–75%), and 3 (>75%). The bone inflammation scores were then averaged for each animal. Bone loss, as defined by the percentage loss of trabecular and/or cortical bone, was scored for each vertebral body in the section; 0 (no bone loss), 1 (<25%), 2 (25–75%), and 3 (>75%). The bone loss scores were then averaged for each animal. TRAP-stained slides were scored to assess osteoclast number. For each TRAP stained section two 400× fields were imaged and analyzed with ImageJ software.

Immunoblotting. Immunoblotting was performed as previously described using anti-IL-1β clone D3H1Z (Cell Signaling), anti-caspase-1 p10 (M-20) antibodies (Santa Cruz Biotechnology), and anti-GAPDH (Calbiochem and Cell Signaling) antibodies (27).

BM-Derived Macrophages and Neutrophils. BMDMs were produced as described previously (27). Briefly, BM cells were collected and cultured with DMEM media (Mediatech) containing 10% (vol/vol) heat-inactivated FBS, penicillin and streptomycin, L-glutamine, and 20% (vol/vol) L929 cell-conditioned media for 6–7 d. Neutrophils were isolated from BM cells by Percoll gradient centrifugation as described previously (31); 85% purity was achieved as assessed by Wright-Geimsa staining.

In Vitro Stimulation. BM cells, BMDMs, or neutrophils were LPS-primed (50 ng/mL *Escherichia coli* serotype 0111:B4 LPS; Invivogen) for 3–4 h and then challenged with 5 mM ATP (Sigma), 50 μg/cm^2 silica (Min-U-Sil-5; Pennsylvania Glass Sand Corporation), or the *P. aeruginosa* PAK strain (multiplicity of infection 1:1). IL-1β secreted into the supernatant was assessed by ELISA (R&D Systems).

ACKNOWLEDGMENTS. We thank Richard Flavell, John Bertin, David Chaplin, and Millennium Pharmaceuticals for providing knockout mice, and William Nauseef for helpful discussion. This work was supported by National Institutes of Health Grants R01 AR059703 (to S.L.C., A.G.B., T.L.B., F.S.S., and P.J.F.), R01 AI087630 (to F.S.S.), R01 AI104706 (to S.L.C.), T32 AI007485 (to J.R.J.), and T32 AI007260 (to S.P.W.), an Edward Mallinckrodt, Jr. Foundation scholarship (to F.S.S.), an Asthma and Allergy Foundation of America fellowship (to S.L.C.), and Care for Kids (P.J.F.).

1. Ferguson PJ, Sandu M (2012) Current understanding of the pathogenesis and management of chronic recurrent multifocal osteomyelitis. *Curr Rheumatol Rep* 14(2): 130–141.
2. Ferguson PJ, El-Shanti HI (2007) Autoinflammatory bone disorders. *Curr Opin Rheumatol* 19(5):492–498.
3. Aksentijevich I, et al. (2009) An autoinflammatory disease with deficiency of the interleukin-1-receptor antagonist. *N Engl J Med* 360(23):2426–2437.
4. Herlin T, et al. (2013) Efficacy of anti-IL-1 treatment in Majeed syndrome. *Ann Rheum Dis* 72(3):410–413.
5. Majeed HA, Al-Tarawna M, El-Shanti H, Kamel B, Al-Khalaileh F (2001) The syndrome of chronic recurrent multifocal osteomyelitis and congenital dyserythropoietic anaemia. Report of a new family and a review. *Eur J Pediatr* 160(12):705–710.
6. Ferguson PJ, et al. (2006) A missense mutation in pstpip2 is associated with the murine autoinflammatory disorder chronic multifocal osteomyelitis. *Bone* 38(1):41–47.
7. Grosse J, et al. (2006) Mutation of mouse Mayp/Pstpip2 causes a macrophage autoinflammatory disease. *Blood* 107(8):3350–3358.
8. Byrd L, Grossmann M, Potter M, Shen-Ong GL (1991) Chronic multifocal osteomyelitis, a new recessive mutation on chromosome 18 of the mouse. *Genomics* 11(4): 794–798.
9. Chitu V, et al. (2009) Primed innate immunity leads to autoinflammatory disease in PSTPIP2-deficient cmo mice. *Blood* 114(12):2497–2505.
10. Ting JP, Kastner DL, Hoffman HM (2006) CATERPILLERs, pyrin and hereditary immunological disorders. *Nat Rev Immunol* 6(3):183–195.
11. Agostini L, et al. (2004) NALP3 forms an IL-1beta-processing inflammasome with increased activity in Muckle-Wells autoinflammatory disorder. *Immunity* 20(3):319–325.
12. Leemans JC, Cassel SL, Sutterwala FS (2011) Sensing damage by the NLRP3 inflammasome. *Immunol Rev* 243(1):152–162.
13. Hazuda DJ, Strickler J, Kueppers F, Simon PL, Young PR (1990) Processing of precursor interleukin 1 beta and inflammatory disease. *J Biol Chem* 265(11):6318–6322.
14. Mizutani H, Schechter N, Lazarus G, Black RA, Kupper TS (1991) Rapid and specific conversion of precursor interleukin 1 beta (IL-1 beta) to an active IL-1 species by human mast cell chymase. *J Exp Med* 174(4):821–825.
15. Schönbeck U, Mach F, Libby P (1998) Generation of biologically active IL-1 beta by matrix metalloproteinases: A novel caspase-1-independent pathway of IL-1 beta processing. *J Immunol* 161(7):3340–3346.
16. Kono H, Orlowski GM, Patel Z, Rock KL (2012) The IL-1-dependent sterile inflammatory response has a substantial caspase-1-independent component that requires cathepsin C. *J Immunol* 189(7):3734–3740.

17. Joosten LA, et al. (2009) Inflammatory arthritis in caspase 1 gene-deficient mice: Contribution of proteinase 3 to caspase 1-independent production of bioactive interleukin-1beta. *Arthritis Rheum* 60(12):3651–3662.
18. Irmler M, et al. (1995) Granzyme A is an interleukin 1 beta-converting enzyme. *J Exp Med* 181(5):1917–1922.
19. Stehlik C (2009) Multiple interleukin-1beta-converting enzymes contribute to inflammatory arthritis. *Arthritis Rheum* 60(12):3524–3530.
20. Fantuzzi G, et al. (1997) Response to local inflammation of IL-1 beta-converting enzyme- deficient mice. *J Immunol* 158(4):1818–1824.
21. Guma M, et al. (2009) Caspase 1-independent activation of interleukin-1beta in neutrophil-predominant inflammation. *Arthritis Rheum* 60(12):3642–3650.
22. Schreiber A, et al. (2012) Neutrophil serine proteases promote IL-1β generation and injury in necrotizing crescentic glomerulonephritis. *J Am Soc Nephrol* 23(3):470–482.
23. Rech J, et al. (2012) Adult-onset Still's disease and chronic recurrent multifocal osteomyelitis: A hitherto undescribed manifestation of autoinflammation. *Rheumatol Int* 32(6):1827–1829.
24. Colina M, et al. (2010) Dysregulation of P2X7 receptor-inflammasome axis in SAPHO syndrome: Successful treatment with anakinra. *Rheumatology (Oxford)* 49(7): 1416–1418.
25. Eleftheriou D, et al. (2010) Biologic therapy in refractory chronic non-bacterial osteomyelitis of childhood. *Rheumatology (Oxford)* 49(8):1505–1512.
26. Kuida K, et al. (1995) Altered cytokine export and apoptosis in mice deficient in interleukin-1 beta converting enzyme. *Science* 267(5206):2000–2003.
27. Sutterwala FS, et al. (2006) Critical role for NALP3/CIAS1/Cryopyrin in innate and adaptive immunity through its regulation of caspase-1. *Immunity* 24(3): 317–327.
28. Glaccum MB, et al. (1997) Phenotypic and functional characterization of mice that lack the type I receptor for IL-1. *J Immunol* 159(7):3364–3371.
29. Horai R, et al. (1998) Production of mice deficient in genes for interleukin (IL)-1alpha, IL-1beta, IL-1alpha/beta, and IL-1 receptor antagonist shows that IL-1beta is crucial in turpentine-induced fever development and glucocorticoid secretion. *J Exp Med* 187(9):1463–1475.
30. Shornick LP, et al. (1996) Mice deficient in IL-1beta manifest impaired contact hypersensitivity to trinitrochlorobenzone. *J Exp Med* 183(4):1427–1436.
31. Boxio R, Bossenmeyer-Pourié C, Steinckwich N, Dournon C, Nüsse O (2004) Mouse bone marrow contains large numbers of functionally competent neutrophils. *J Leukoc Biol* 75(4):604–611.